J. Biochem. 126, 510-519 (1999)

Azide- and Cyanide-Binding to the *Escherichia coli bd*-Type Ubiquinol Oxidase Studied by Visible Absorption, EPR and FTIR Spectroscopies[1]

Motonari Tsubaki,*,†,2 Tatsushi Mogi,‡ and Hiroshi Hori§

Department of Life Science, Faculty of Science, Himeji Institute of Technology, Kamigoori-cho, Akou-gun, Hyogo 678-1297; †Institute for Molecular Science, Okazaki National Research Institutes, Myodaiji, Okazaki, Aichi 444-8585; ‡Department of Biological Sciences, Graduate School of Science, The University of Tokyo, Hongo, Bunkyo-ku, Tokyo 113-0033; and §Division of Biophysical Engineering, Graduate School of Engineering Science, Osaka University, Machikaneyama-cho, Toyonaka, Osaka 560-8351

Received March 23, 1999; accepted June 24, 1999

Cytochrome *bd*-type ubiquinol oxidase contains two hemes *b* (b_{558} and b_{595}) and one heme *d* as the redox metal centers. To clarify the structure of the reaction center, we analyzed *Escherichia coli* cytochrome *bd* by visible absorption, EPR and FTIR spectroscopies using azide and cyanide as monitoring probes for the exogenous ligand binding site. Azide-binding caused the appearance of a new EPR low-spin signal characteristic of ferric iron-chlorin-azide species and a new visible absorption band at 647 nm. However, the bound azide ($^{14}N_3$) anti-symmetric stretching infrared band (2,010.5 cm^{-1}) showed anomalies upon ^{15}N-substitutions, indicating interactions with surrounding protein residues or heme b_{595} in close proximity. The spectral changes upon cyanide-binding in the visible region were typical of those observed for ferric iron-chlorin species with diol substituents in macrocycles. However, we found no indication of a low-spin EPR signal corresponding to the ferric iron-chlorin-cyanide complexes. Instead, derivative-shaped signals at $g=3.19$ and $g=7.15$, which could arise from the heme $d(Fe^{3+})$-CN-heme $b_{595}(Fe^{3+})$ moiety, were observed. Further, after the addition of cyanide, a part of ferric heme *d* showed the rhombic high-spin signal that coexisted with the $g_z=2.85$ signal ascribed to the minor heme b_{595}-CN species. This indicates strong steric hindrance of cyanide-binding to ferric heme *d* with the bound cyanide at ferric heme b_{595}.

Key words: azide, cyanide, EPR, FTIR, *bd*-type ubiquinol oxidase.

In the aerobic respiratory chain of *Escherichia coli*, there are two structurally unrelated terminal ubiquinol oxidases (*1, 2*). Cytochrome *bo* predominates under highly aerated growth conditions while an alternative oxidase, cytochrome *bd*, is synthesized as a major terminal oxidase under microaerobic conditions. Both oxidases catalyze the two-electron oxidation of ubiquinol-8 on the periplasmic side and the four-electron reduction of dioxygen on the cytoplasmic side, respectively, of the cytoplasmic membranes, whereas only cytochrome *bo* exhibits vectorial proton transport (*1, 2*). The molecular mechanism of electron transfer and the chemical reactions of dioxygen in the respiratory terminal oxidases have been of great interest. However, only a little structural information has been obtained for cytochrome *bd*.

Cytochrome *bd* contains two hemes *b* (b_{558} and b_{595}) and one heme *d* (*1, 2*), but no copper ions (*3, 4*). The heme *d* prosthetic group is structurally unique in that it is actually an iron-chlorin derived from an iron-protoporphyrin IX. Pyrrole ring C of the macrocycle is saturated by introducing two hydroxyl groups at the C5 and C6 positions, respectively, in the *trans* configuration (*5, 6*). Such alterations give heme *d* a green color and a very distinct visible absorption spectrum (*7*). Heme *d* is a primary active site for dioxygen-binding and reduction (*1, 2*). In the air-oxidized state, the enzyme exists as an ~70:30 mixture of two stable oxy-forms: the ferrous-oxygenated (Fe^{2+}-O_2) (*8, 9*) and ferryl-oxo (Fe^{4+}=O) species (*1, 10*). A part (~10%) of heme *d* exists in the ferric form and, thus, can be EPR-detectable (*11, 12*). Heme *d* and heme b_{595} are located fairly close to each other (*13*), and may form a heme-heme binuclear reaction center (*14-16*).

Very recently, we found that a fluoride ion can coordinate heme *d* and heme b_{595} in different affinities in the fully oxidized state on the basis of the results of visible and EPR spectroscopies (*17*). The inaccessibility of a fluoride ion to a large part of ferric heme b_{595} in the air-oxidized state, however, suggested the proximity of heme b_{595} and heme *d*. In addition, we established that the rhombic high-spin EPR signal in the fully oxidized state is actually derived from

[1] This work was supported in part by Grants-in-Aid for Scientific Research on Priority Areas (Molecular Biometalics; 10129226 to MT, 08249106 to TM and HH) and for Scientific Research (C) (09833002 to MT, 09680651 to HH) from the Ministry of Education, Science, Sports and Culture of Japan.

[2] To whom correspondence should be addressed. Tel/Fax: +81-791-58-0189, E-mail: tsubaki@sci.himeji-tech.ac.jp

Abbreviation: FTIR, Fourier-transform infrared spectroscopy.

ferric heme *d* (*17*), contrary to the previous assignment, in which the rhombic and axial high-spin EPR signals were ascribed to ferric heme b_{595} and ferric heme *d*, respectively (*18, 19*).

Azide and cyanide anions can form very stable complexes with ferric heme iron and have been used extensively to probe the active site structure of the metal's sixth coordination position in hemoproteins. Heme-azide complexes in protein moieties exhibit a low-spin ground state and an observable spin equilibrium near room temperature (*20*). Whereas heme-cyanide complexes adopt a pure low-spin state irrespective of temperature. Fourier-transform infrared (FTIR) spectroscopy has been used to probe the environment of the active center through detection of the vibrational modes of these ligands (*21, 22*), and the thermal spin equilibria of azide derivatives of hemoglobin and myoglobin have been studied through analyses of two anti-symmetric stretching bands of bound azide (*23*). On the other hand, EPR spectroscopy is particularly suitable for the investigation of the electronic structure of heme iron when various heme ligands are coordinated (*24-27*). Indeed, Walker and coworkers proposed that low-spin ferric-chlorin species have a novel $(d_{xz}, d_{yz})^4(d_{xy})^1$ ground state, very different from low-spin ferric-porphyrin species, on the basis of unusual EPR spectra for low-spin ferric chlorins (*28*). In the present study, we applied EPR, FTIR and visible absorption spectroscopies, utilizing azide and cyanide as monitoring probes for the active site structure of *E. coli* cytochrome *bd*.

MATERIALS AND METHODS

Preparation of Cytochrome bd—The enzyme was purified from overproducing strain GR84N/pNG2 (*cyo*$^+$ *cydA2/cyd*$^+$), a generous gift from R.B. Gennis, as described previously (*16*), and was stored at −80°C in 50 mM Na-phosphate buffer (pH 7.4) containing 0.1% sucrose monolaurate 1200 (Mitsubishi-Kagaku Foods, Tokyo). The concentration of the enzyme was calculated from the extinction coefficient in the air-oxidized state at 414 nm ($\varepsilon = 223\ mM^{-1} \cdot cm^{-1}$), which is based on the heme B content determined by the pyridine ferrohemochromogen method (*16*).

The fully oxidized form was prepared as follows. The air-oxidized dioxygen-bound cytochrome *bd* in a small glass tube with a rubber septum was deoxygenated under flowing pure argon gas passed through two needles (one as an inlet and the other as an outlet). Then, sodium dithionite was added anaerobically, and the mixture was incubated on ice for 30 min. Then, an excess amount of a (deoxygenated) sodium ferricyanide solution was added anaerobically. The sample was stood on ice for an additional 30 min. The fully oxidized sample was gel-filtered in 50 mM Na-phosphate buffer (pH 7.4) containing 0.1% sucrose monolaurate 1200 through an Ampure SA cartridge column (Amersham). Visible absorption spectra were then obtained.

The samples for the EPR and FTIR spectroscopies were prepared essentially as previously described (*16, 27*). A NaN_3 solution (200 mM) was added, using an air-tight microsyringe, to the concentrated samples in a substoichiometric amount (final concentration, 0.5 mM) to avoid interference from the free azide bands (Fig. 4 and Table II). The following sodium azide isotopes were used: $Na^{14}N_3$ (natural abundance; Nacalai Tesque, Kyoto); $Na^{15}N^{14}N^{14}N$ (99 atom% ^{15}N; ICON, Mt. Marion, NY); $Na^{15}N^{15}N^{14}N$ (95 atom% ^{15}N; Berlin Chemie, Berlin), and $Na^{15}N_3$ (95 atom% ^{15}N; Laboratorien Berlin-Adlershof GmbH, Berlin). A KCN stock solution (1 M) was added similarly at a final concentration of 10 mM to the air-oxidized, fully-oxidized, and azide-treated forms.

Visible and Infrared Spectroscopies—Visible absorption spectra were measured with a Shimadzu UV-2200 or UV-2400PC spectrophotometer (Shimadzu, Kyoto) or a UVIKON 922 spectrophotometer (Kontron Instruments). Infrared absorption spectra were measured at 2°C with a double beam FTIR spectrophotometer (Perkin Elmer, Model 1850) as previously described (*27*). For infrared spectroscopy, typically, 400 ready-made scanning cycles of data accumulations at 4 cm^{-1} resolution were performed and the data were analyzed. Absolute visible spectra of the enzyme in infrared cells with a 51 μm path length were measured at room temperature with the Shimadzu UV-2400PC spectrophotometer before and after FTIR measurements.

EPR Spectroscopy—EPR measurements were carried out at X-band (9.23 GHz) microwave frequency with a Varian E-12 EPR spectrometer equipped with an Oxford flow cryostat (ESR-900), as previously described (*29*).

RESULTS

Visible Absorption Spectroscopic Study—In the past, only a few studies have been conducted on the interaction of azide ions with the air-oxidized cytochrome *bd*. This is apparently due to the very stable coordination of dioxygen to ferrous heme *d*, which obstructs the oxidation of heme *d* with oxidants such as ferricyanide. Indeed, the addition of ferricyanide (final, 10 mM) to the air-oxidized enzyme at room temperature did not cause any reduction in the intensity of the 647 nm absorption characteristic of the ferrous heme *d*-dioxygen species nor the 680 nm band characteristic of the heme *d*-oxoferryl species. To obviate the protective effect of the bound dioxygen (or oxoferryl species) and the heterogeneity at the reaction center, we first removed free and bound dioxygen with an excess amount of sodium dithionite. After complete reduction of the metal centers, an excess amount of ferricyanide was added anaerobically. The visible spectrum in the fully oxidized state, thus obtained, could be characterized by the unresolved Soret band centered at 413 nm (not shown), and weaker bands centered at 535, 595, 645, and 743 nm (Fig. 1A). Stepwise addition of azide to the fully oxidized enzyme caused a gradual increase in the absorbance at 647 nm, with a simultaneous decrease at 743 nm (Fig. 1A). The weak band at 595 nm also decreased during the titration (Fig. 1A). The apparent K_d-value for azide-binding was calculated based on the changes in absorption at 647 nm and was found to be 3.4 mM (Fig. 1A, inset). We found that the addition of azide to the air-oxidized enzyme caused a similar spectral change, but the extent was much smaller. The K_d value for the air-oxidized enzyme was 3.6 mM, *i.e.*, it was almost identical.

We found previously that a fluoride ion can coordinate to both ferric heme *d* and ferric heme b_{595} in different affinities in the fully oxidized state (*17*). The K_d-value for the fluoride-binding to ferric heme *d* was found to be 36

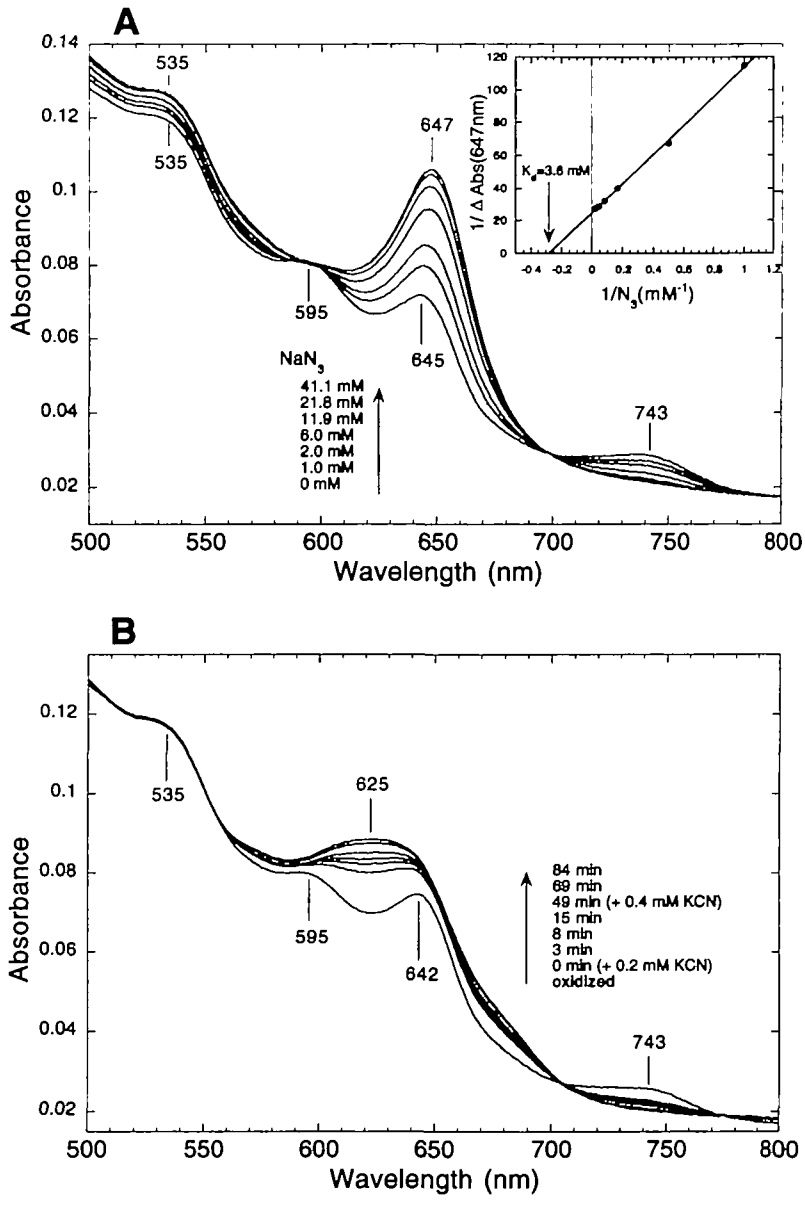

Fig. 1. **Visible absorption spectral changes of fully oxidized cytochrome *bd* upon the addition of azide (A) and cyanide (B).** The inset in panel (A) shows a double reciprocal plot of the absorbance changes at 647 nm upon the addition of azide. The conditions for measurements were as follows: temperature, 20°C; sample concentration, 4.18 μM in 50 mM Na-phosphate buffer (pH 7.4) containing 0.1% sucrose monolaurate 1200. (A) Azide was added to the oxidized enzyme as sodium azide, at final concentrations of 1.0, 2.0, 6.0, 11.9, 21.8, and 41.1 mM. (B) Cyanide was added to the oxidized enzyme as potassium cyanide, at a final concentration of 0.20 mM, and the spectral changes were recorded just after (0 min), and 3, 8, 15 and 49 min after the addition. Then, 0.40 mM cyanide was added additionally and the spectrum was recorded (at 49 min after the first addition). At 84 min after the first addition, the spectrum was finally recorded and the spectral change was found to be completed.

mM at pH 7.4. The azide-binding to ferric heme *d* was examined in the presence of a saturating amount of fluoride ions (580 mM). The bound fluoride ions were almost completely replaced with azide ions, as judged on visible absorption spectroscopy, and the apparent K_d value was calculated (based on the changes in absorbance at 647 nm) to be 41 mM at pH 7.4. Thus, fluoride and azide ions compete for the same, or partially overlapped, active site, *i.e.*, ferric heme *d*.

We examined the binding of other halide or pseudohalide ions to ferric heme *d*. The thiocyanate (SCN^-) ion was found to bind to ferric heme *d* with an apparent K_d-value of 141 mM at pH 7.4 (based on the changes in absorbance at 625 nm) (spectra not shown). The addition of cyanate (OCN^-) ions caused a slight spectral change similar to that caused by thiocyanate ions, but further addition caused denaturation. Therefore, we did not further pursue the binding of cyanate ions. Other halide ions, including Cl^-, Br^-, and I^-, showed no indication of binding.

The addition of cyanide (CN^-) ions to the fully oxidized enzyme caused the rapid disappearance of the 743, 643, and 595 nm bands, and the appearance of a broad band at 625 nm (Fig. 1B). The visible spectral change after the addition of cyanide to the air-oxidized state was very slow, suggesting replacement of bound dioxygen with cyanide or oxidation of ferrous heme *d*. The spectrum after overnight incubation showed a broad band centered around 625 nm, very similar to that obtained for the fully oxidized form.

EPR Spectroscopic Study—In both the air-oxidized and fully oxidized states, cytochrome *bd* showed two kinds of low-spin signals [Fig. 2, A and B, spectra (a), and Table I]. The major one was the $g_z = 2.474$ species ($g_y \sim 2.33$, $g_x = 1.845$, $g_{x'} = 1.814$), and the other was a peculiar $g_z = 2.605$ species (g_y, g_x, uncertain). Considering the difference in enzyme concentration, the intensities of the low-spin EPR signals increased about 6.5-fold (Fig. 2, A and B), whereas those of the *g*6 high-spin signals increased about 2.5 fold (Fig. 3, A and B), upon oxidation of the air-oxidized

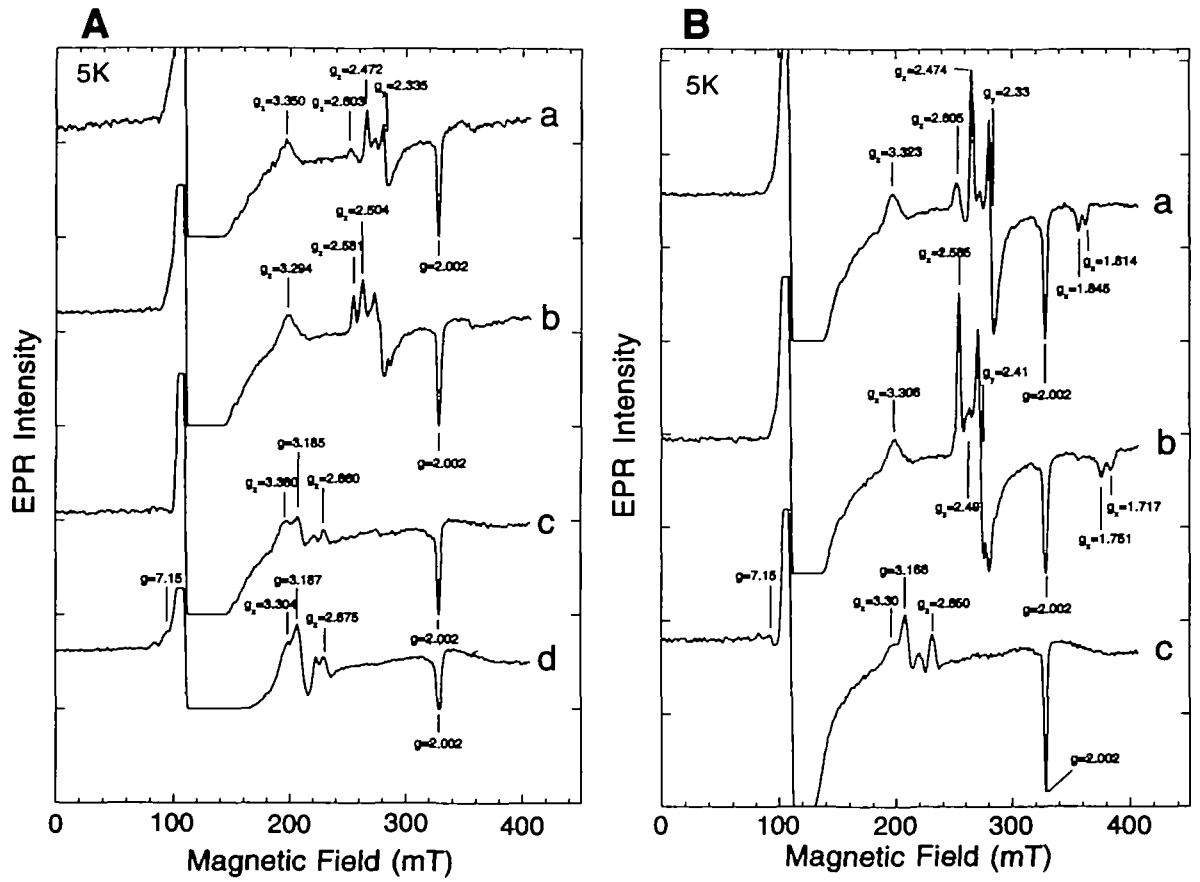

Fig. 2. **(Panel A) Low-spin EPR spectra of cytochrome *bd* in the air-oxidized state (a), after the addition of 50 mM azide (after 1 h incubation on ice) (b), after further addition of 10 mM cyanide (after 30 min incubation on ice) (c), and after overnight incubation with cyanide (10 mM) on ice without azide (d). (Panel B) Low-spin EPR spectra of cytochrome *bd* in the fully oxidized state (a), after the addition of 50 mM azide (after 1 h incubation on ice) (b), and after further addition of 10 mM cyanide (after 30 min incubation on ice) (c).** The conditions for measurements were as follows: microwave frequency, 9.22 GHz; incident microwave power, 5 mW; 100-kHz field modulation width, 0.5 mT; temperature, 5 K. The ordinate of spectrum (d) in panel A was expanded 2-fold for clarification. Sample concentrations; (panel A) 0.577 mM, (panel B) 0.203 mM, both in 50 mM Na-phosphate buffer (pH 7.4) containing 0.1% sucrose monolaurate 1200.

TABLE I. **EPR signals derived from the air-oxidized and fully oxidized cytochrome *bd* in the absence and presence of azide and cyanide ions at 5 K.**

Assignment	Subspecies	*g*-values		
Low-spin signals				
$d(Fe^{3+})$-OH	(1)	$g_x=2.474$	$g_y=2.33$	$g_x=1.814$
	(2)			$g_{x'}=1.845$
$d(Fe^{3+})$-N_3	(1)	$g_x=2.585$	$g_y=2.41$	$g_x=1.717$
	(2)			$g_{x'}=1.751$
	(3)	$g_x=2.504$	?	?
$b_{595}(Fe^{3+})$-OH(?)		$g_x=2.605$	?	?
$b_{595}(Fe^{3+})$-CN		$g_x=2.859$	?	?
$b_{558}(Fe^{3+})$		$g_x=3.30$	?	?
High-spin signals				
$d(Fe^{3+})$	(rhombic)	$g_x=6.3$	$g_y=5.54$	$g_x=2.002$
$b_{595}(Fe^{3+})$	(axial)	$g_\perp=6.08$	$g_{//}=2.00$	
$d(Fe^{3+})$-CN-$b_{595}(Fe^{3+})$		$g=7.15$	$g=3.189$	

enzyme.

The addition of azide (50 mM) to the air-oxidized enzyme caused the disappearance of these low-spin EPR signals. Instead, two kinds of new low-spin EPR signals appeared ($g_z=2.581$ and 2.504 species), indicating the formation of the ferric heme *d*-azide species [Fig. 2A, spectrum (b), and Table I]. The addition of azide to the fully oxidized enzyme caused a similar spectral change; but the relative intensities of the two ferric heme *d*-azide low-spin species were very different, the intensity of the $g_z=2.581$ species being much stronger than that of the $g_z=2.504$ species [Fig. 2B, spectrum (b)]. The observed spectral change in the low-spin region was similar to that observed previously for membrane vesicles containing cytochrome *bd* (*11*). Upon the addition of azide to the fully oxidized enzyme, the in-plane *g*-anisotropy of high-spin species increased (broadening of the *g*6 signal toward lower magnetic field and a shift of a trough from $g=5.66$ to 5.61) [Fig. 3, A and B, spectra (b)]. Consistent with this, the high-spin *g*2 signal showed a significant broadening towards higher magnetic field (Fig. 3C), indicating that the formation of a new heme *d*-azide high-spin species occurred also.

The addition of cyanide (10 mM) to the azide-treated fully oxidized sample caused the complete loss of the ferric heme *d*-azide low-spin signals and the appearance of unusual features in the $g=3.2$-2.8 region, which overlapped the $g_z=3.30$ signal derived from ferric b_{558} low-spin species at 5 K [Fig. 2, A and B, spectra (c), and Table I].

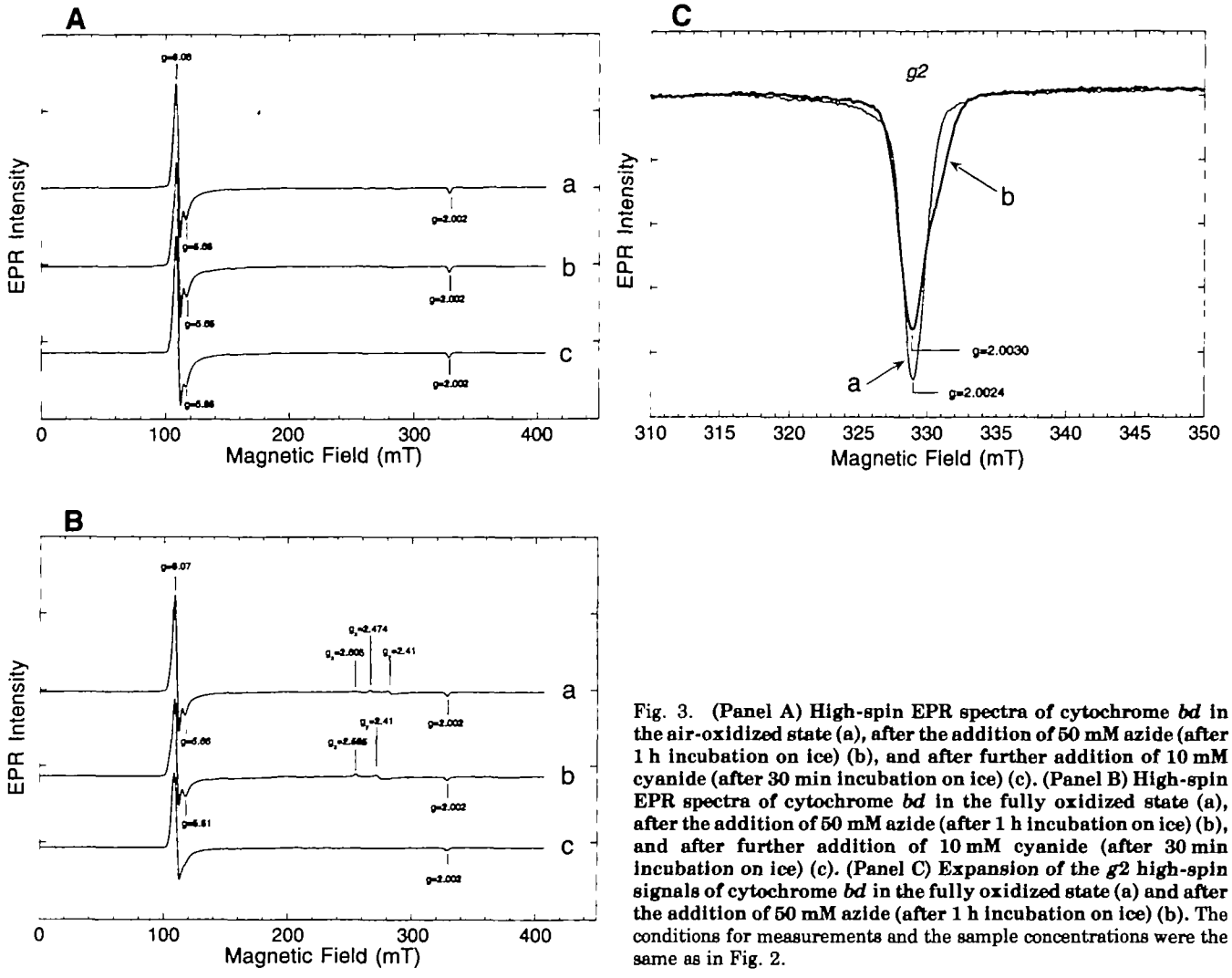

Fig. 3. **(Panel A) High-spin EPR spectra of cytochrome *bd* in the air-oxidized state (a), after the addition of 50 mM azide (after 1 h incubation on ice) (b), and after further addition of 10 mM cyanide (after 30 min incubation on ice) (c). (Panel B) High-spin EPR spectra of cytochrome *bd* in the fully oxidized state (a), after the addition of 50 mM azide (after 1 h incubation on ice) (b), and after further addition of 10 mM cyanide (after 30 min incubation on ice) (c). (Panel C) Expansion of the *g*2 high-spin signals of cytochrome *bd* in the fully oxidized state (a) and after the addition of 50 mM azide (after 1 h incubation on ice) (b).** The conditions for measurements and the sample concentrations were the same as in Fig. 2.

Indistinguishable signals were observed upon the addition of cyanide alone to the fully oxidized enzyme. Similar signals were also obtained upon the addition of cyanide alone to the air-oxidized enzyme, as previously reported (*16*). The intensity of the peculiar $g=3.19$ signal became much stronger during overnight incubation with cyanide [Fig. 2B, spectrum (d)]. We confirmed our previous observation that the $g=3.19$ signal was not a usual g_z component of low-spin ferric heme *d*-cyanide species, but had a clear derivative-like line shape [Fig. 2B, spectra (c, d)]. In addition, we noticed another peculiar signal at $g=7.15$ that is specific to the cyanide species [Fig. 2A, spectrum (d), and Fig. 2B, spectrum (c)] and may have a similar origin to the $g=3.19$ species. An additional signal at $g=2.85$ seems to have a different origin from the $g=3.19$ signal, considering the variation in relative intensity, as shown in Fig. 2B [spectra (c, d)]. A decrease in the rhombic high-spin signal (*i.e.*, the $g=5.66$ signal) was apparent upon the addition of cyanide to the air-oxidized enzyme [Fig. 3A, spectrum (c)]. Such a decrease was more significant for the fully oxidized enzyme, where the rhombic high-spin signal became very weak just after the addition of cyanide [Fig. 3B, spectrum (c)]. At the same time, the intensities of both the $g=3.19$ and $g=2.85$ signals appeared to be almost full. Overnight incubation of the air-oxidized enzyme in the presence of cyanide lead to a similar spectrum to that of the oxidized enzyme.

The addition of thiocyanate to the fully oxidized enzyme caused spectral changes in both the high- and low-spin regions. Two types of low-spin species (one species with $g_z=2.731$, $g_y=2.313$, and $g_x=1.819$; the other with $g_z=2.576$, $g_y=2.435$, and $g_x=1.839$) were newly formed. The in-plane *g*-anisotropy of the high-spin signal (the $g=5.64$ species) became much greater (spectra not shown).

FTIR Spectroscopic Study—FTIR spectra of the air-oxidized enzyme in the presence of a substoichiometric amount of azide (0.5 mM) did not show any infrared band derived from the bound species except for a free azide antisymmetric stretching band centered at 2,048 cm^{-1}, indicating that the amount of the heme $d(Fe^{3+})$-N_3 low-spin species is very small and is lower than the detectable level. The addition of azide to the fully oxidized enzyme caused the appearance of a new band at 2,010.5 cm^{-1} [Fig. 4(a)]. This band showed shifts to 1,991, 1,947, and 1,945 cm^{-1} upon substitution with $^{15}N^{14}N^{14}N$, $^{15}N^{15}N^{14}N$, and $^{15}N_3$, respectively [Fig. 4, (b), (c), and (d), and Table II]. All these bound azide bands disappeared upon the addition of cyanide ($^{12}C^{14}N$; 10 mM), leaving the 2,161 cm^{-1} cyanide-

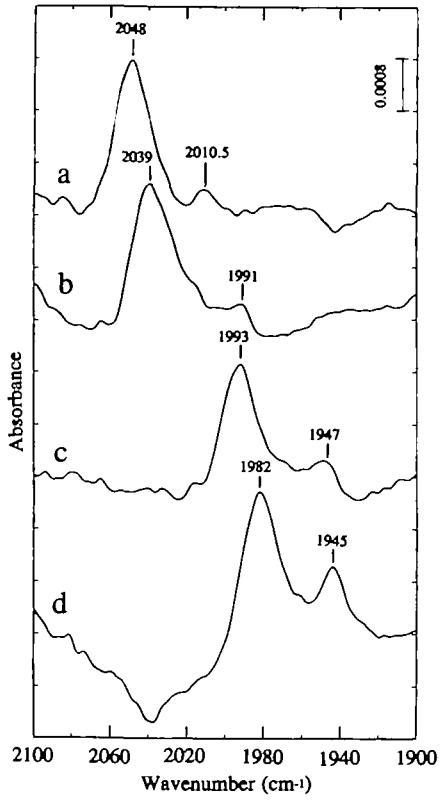

Fig. 4. **FTIR spectra of cytochrome *bd* in the fully oxidized state in the presence of 0.50 mM each of $^{14}N_3$ (a), $^{15}N^{14}N^{14}N$ (b), $^{15}N^{15}N^{14}N$ (c), and $^{15}N_3$ (d) in the 2,100-1,900 cm^{-1} region.** The conditions for measurements were as follows: spectral resolution, 4.0 cm^{-1}; spectral accumulation, 400 cycles; temperature, 2°C. Sample concentration, 0.941 mM, in 50 mM Na-phosphate buffer (pH 7.4) containing 0.1% sucrose monolaurate 1200.

bridging band (*16*) and corresponding free azide bands, respectively. These observations suggest that the sites for azide-binding and cyanide-binding are identical or, at least, partially overlapped. It is of note that there is no splitting of azide antisymmetric stretching vibrations for the two nonsymmetrically ^{15}N-labeled azides. Although we did not analyze the azide-binding affinity of ferric heme *d* by FTIR spectroscopy, the affinity seemed rather high since only a sub-millimolar concentration of azide was enough to cause the appearance of the infrared bands.

The addition of cyanide ($^{12}C^{14}N$; 10 mM) alone to the fully oxidized enzyme caused the appearance of a cyanide band at 2,161 cm^{-1}. This band showed expected shifts upon cyanide isotope substitutions, as previously noted for the air-oxidized enzyme (*16*). An FTIR study on thiocyanate-binding was not conducted due to the very low binding affinity.

DISCUSSION

Visible Absorption Spectroscopy—Oxidation of the air-oxidized cytochrome *bd* caused the appearance of two characteristic visible bands at 743 and 595 nm assignable to ferric heme *d* in the high-spin state (*17*) based on the similarity of its peak location to those of various iron-chlorin containing hemoproteins and model complexes (*30-32*). The 642 nm band in the fully oxidized spectrum is not due to the residual ferrous heme *d*-dioxygen species but rather may be ascribed to ferric heme b_{595} (*17, 33*). Both the 743 and 595 nm bands completely disappeared upon the addition of azide to the fully oxidized enzyme, and a new band appeared at 647 nm. Indeed, various ferric iron-chlorin-azide complexes exhibit a band around the 620-630 nm region (*31, 34, 35*). The addition of excess azide to the pre-formed fluoride- or thiocyanate-complex caused the formation of a band at 647 nm, indicating the complete replacement of the bound ligands. All these spectral data suggest that ferric heme *d* is a primary binding site for azide ions, and fluoride and thiocyanate ions bind at the same or, at least, a partially overlapping site [Fig. 5(c, d)]. The inability of the binding of other larger halide ions to ferric heme *d* suggests that the binding site for exogenous ligands is rather small, *i.e.*, just enough to accommodate two fluoride ions (or a molecular ion comprising atoms in the second period). The effective size of the molecular ions (azide, cyanate, and thiocyanate ions) may not be much different from those in the neutral state due to the dilution of a single negative charge on the whole molecule. It should be noted that the thiocyanate ion is known to coordinate to an iron through the terminal nitrogen atom and, therefore, the bulkiness of a sulfur atom in the other terminal may be not so important for the coordination.

TABLE II. **Bound azide antisymmetric infrared stretching vibrations of fully oxidized cytochrome *bd*.**

Azide	Frequency (cm^{-1})	
	Free N_3	Bound N_3
$^{14}N_3$	2,048	2,010.5
$^{15}N^{14}N^{14}N$	2,039	1,991
$^{15}N^{15}N^{14}N$	1,993	1,947
$^{15}N_3$	1,982	1,945

On the other hand, the addition of cyanide to the fully oxidized enzyme caused the disappearance of the characteristic three bands (at 743, 642, and 595 nm) altogether, indicating that both heme *d* and heme b_{595} participate in cyanide-binding. However, as reported previously (*16*) and confirmed in the present study, there is only one major cyanide stretching infrared band (at 2,161 cm^{-1}) after the full formation of the cyanide complex. These results are consistent with our proposal that a cyanide ion binds to ferric heme *d* and heme b_{595} as a bridging ligand [Fig. 5(d)] (*16*). As we will discuss below, the present EPR data are also consistent with this view.

Several visible spectroscopic studies on cyanide-binding to hemoproteins containing iron-chlorin prosthetic groups have been reported. The hemoproteins containing a chlorin macrocycle without direct oxygen group substituents at pyrrole rings tend to exhibit an absorption band around 580-600 nm for their ferric-cyanide species (*31, 32, 35, 36*). On the other hand, a directly-attached hydroxyl- (*i.e.*, iron-photoprotoporphyrin or heme *d*) or oxo-group(s) (*i.e.*, heme d_1) at the chlorin macrocycle causes a red shift of the absorption maximum to the region of 630 to 650 nm (Hori and Sono, unpublished) (*37-39*). All these ferric-iron-chlorin-cyanide species, however, showed EPR signals characteristic of the 6-coordinated low-spin species irrespective of the peak location of the visible absorption band (see later discussion on EPR spectroscopy). Thus, the broad band observed at 625 nm (Fig. 1D) is consistent with the notion

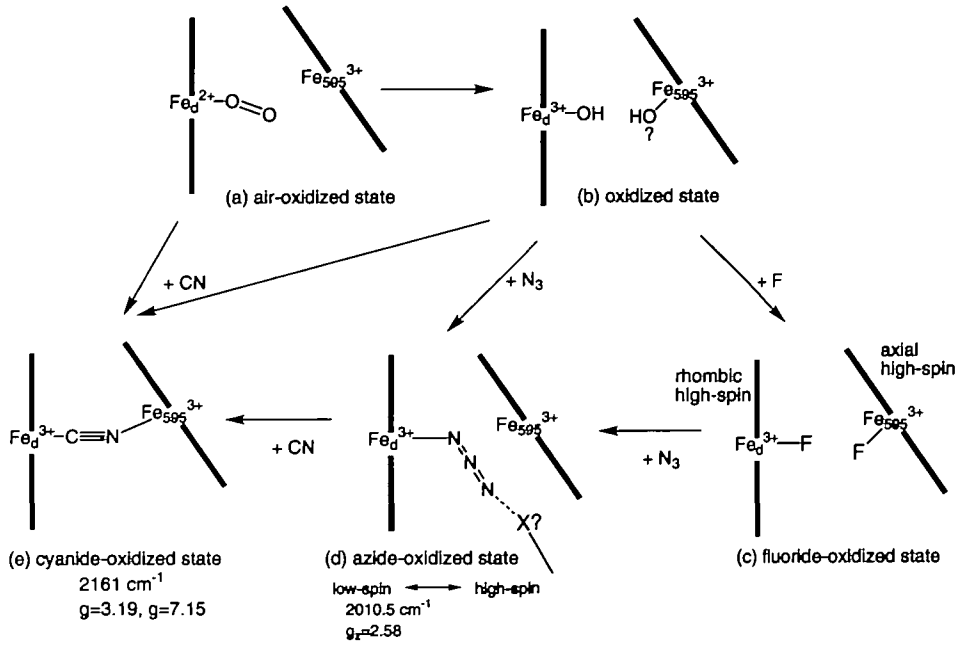

Fig. 5. Schematic representation of the active site structure of cytochrome *bd* and its interaction with exogenous ligands.

that the primary binding site for cyanide is ferric heme *d* and the resultant ferric heme *d*-cyanide species should be intrinsically in a low-spin state.

FTIR Spectroscopy—In the air-oxidized state, the addition of azide in a substoichiometric amount did not cause any bound azide infrared band except for the one due to free azide ions. Visible and EPR spectroscopic studies, however, showed that at least some part of ferric heme *d* binds azide ions. Since ferric heme *d* accounts for only 10% of the total heme *d* population in the air-oxidized state (*11*), the population of the low-spin species, as evidenced by EPR spectroscopy, is too low to be detected as a distinct infrared band.

Upon the oxidation of ferrous heme *d*, a major part of heme *d* becomes accessible to azide [Fig. 5(b, d)], as evidenced by the visible spectral change. This leads to the appearance of a new broad azide band at 2,010.5 cm^{-1}. This azide band showed downward frequency shifts upon isotopic substitutions with ^{15}N (Table II). This new band, however, has a very different character from those of the usual low-spin (or high-spin) ferric heme-azide species. First, if an azide ion ligates to ferric heme *d* in the usual coordination *via* terminal nitrogen atom, the azide antisymmetric stretching band should become split when nonsymmetrically ^{15}N-labeled azides are used, irrespective of the spin state (*i.e.*, both in the low- and high-spin states) (*22*). The extent of the splitting depends on the geometry of the azide-binding to the metal; for a low-spin state, it is typically around 12-16 cm^{-1}, whereas for a high-spin state, it is around 9-12 cm^{-1}, for ^{15}N^{14}N^{14}N species (Tsubaki, M., unpublished). Second, the bound azide stretching frequency (2,010.5 cm^{-1}) itself is unusually low. Ferric heme-azide species usually give two type of antisymmetric stretching vibrations around 2,023 and 2,046 cm^{-1} for the low- and high-spin species, respectively (*23, 40*). Heme-azide species with a much lower stretching frequency can be observed for some mutant myoglobins in which the distal His residue is replaced with Thr or Ile (*41*). Azide species bound to the heme-copper binuclear center of cytochrome *c* oxidase also exhibit such unusually low stretching frequencies (*22*). There are several possible explanations for the anomalies of this azide species. As one possibility, an azide ion may bind in a bridging configuration between the two heme irons, just like we proposed for the cyanide-binding (*16*). However, this scheme cannot explain the appearance of the ferric heme *d*-azide low-spin EPR signals, since such a bridging configuration will cause significant anomalies in the EPR spectra [*i.e.*, disappearance of EPR signals or appearance of unusual EPR signals derived from a spin-exchanged coupled species, as observed for the azide-bridged heme-copper oxidases (*27, 42, 43*)]. However, if the azide-bridging configuration is not so rigid, the bond between azide and heme b_{595} may be easily broken upon freezing, leaving heme *d*-azide low-spin and 5-coordinated heme b_{595} high-spin species. In this case, we will not see any anomalies in the EPR spectra, as shown in the present study. As an alternative possibility, the coordinated azide ion may be stabilized with a protein residue(s) [denoted by X? in Fig. 5(d)] in the active site pocket to compensate for the inequivalence of the two N-N bonds of the bound azide (*44, 45*). Indeed the pattern of the azide isotopic shifts observed in the present study was very different from those of heme-copper oxidases in the azide-bridging configuration (*22, 46*), indicating an intrinsic difference in the azide-binding.

The intensity of the 2,010.5 cm^{-1} band was only a minor part of the whole azide infrared band, as shown in Fig. 4. The high-spin heme *d*-azide species, if any, might be overlapped by the strong infrared band derived from free azide ions. EPR data suggest that this is indeed the case (see discussion in the next section).

EPR Spectroscopy—In the air-oxidized state, there were two ferric low-spin species (the major g_z=2.472 species and the peculiar g_z=2.603 species). The former is apparently due to heme *d*, whereas the origin of the latter species is not clear. It may be derived from heme b_{595}-hydroxide. It

should be mentioned, however, that ferric heme *d* in the low-spin state accounts for only a minor part of the total heme *d* population in the air-oxidized state. A major part is either in a ferrous oxygenated [Fig. 5(a)] or ferryl-oxo state, both being EPR-invisible. Oxidation of the air-oxidized enzyme caused extensive intensification of the low-spin signals (both the $g_z = 2.474$ and 2.605 species) and the appearance of two g_x components (*i.e.*, $g_x = 1.814$ and $g_{x'} = 1.845$). Although we postulated that the $g_z = 2.474$ species is actually composed of two species, one gives $g_x = 1.814$ and the other gives $g_{x'} = 1.845$ (in this case, the $g_z = 2.605$ species is an unusual one showing no g_x component in the spectra), and the $g_x = 1.814$ component may be derived from the $g_z = 2.605$ species. The addition of azide to the air-oxidized enzyme caused a clear spectral change in the low-spin region. Both the $g_z = 2.472$ and 2.603 species disappeared and two new ferric low-spin species ($g_z = 2.581$ and 2.505 species) were formed. These new low-spin species can be explained as an exchange of the heme *d* ligand from hydroxide to azide [Fig. 5(b, d)]. The hydroxide ligand at heme b_{595} may be expelled by the azide-binding at heme *d*. Although the addition of azide to the fully oxidized enzyme seemed to cause the formation of only the $g_z = 2.585$ species, the presence of two g_x components (*i.e.*, $g_x = 1.717$ and 1.751) suggests that the $g_z = 2.585$ species is actually composed of two species. Thus, the heterogeneity at the reaction center in the air-oxidized state could not be abolished completely by the full oxidation.

The observed *g*-values for the ferric heme *d*-azide species were very similar to those of other ferric iron-chlorin-azide species (*31, 35, 47, 48*). In the high-spin EPR signal region, the anisotropic signal at $g = 5.66$ ascribed to ferric heme *d* (*17*) showed a shift to $g = 5.61$ upon the addition of azide. The high-spin *g*2 signal also showed broadening to higher magnetic field. These observations indicate that a considerable part of the ferric heme *d*-azide species adopted a rhombic high-spin state at low temperature.

The addition of cyanide to the fully oxidized or the azide-bound fully oxidized enzyme caused a dramatic change in EPR spectra in both the low- and high-spin signal regions. The appearance of the peculiar $g = 3.19$ signal is indicative of the heme *d*-C-N-heme b_{595} bridging species at the active center [Fig. 5(e)], as previously suggested (*16*). Another peculiar signal at $g = 7.15$ is likely to have a similar origin to the $g = 3.19$ species. It has been suggested that the features in the $g = 3.2$-2.8 region are due to the ferric heme *d*-cyanide species (*19, 49*). However, EPR studies on hemoproteins containing a wide variety of iron-chlorin prosthetic groups showed that such a possibility is unlikely. Various ferric iron-chlorin-cyanide species [including heme *d* (*50*), iron-photoprotoporphyrin IX (Hori and Sono, unpublished), iron-octaethylchlorin (*35*), sulfheme (*31*), heme d_1, and siroheme] showed g_z values in the relatively narrow range of 2.71 to 2.34. On this basis, our previous assignment of the $g = 2.82$ and $g = 2.96$ species (the latter appears only transiently upon reduction of the preformed heme *d*(Fe^{3+})-C-N-heme b_{595}(Fe^{3+}) bridging species) (*16*) needs reconsideration. The $g = 2.82$ (the $g = 2.85$ species in the present study) is more likely to be due to the g_z-component of the ferric heme b_{595}-cyanide species. A part of cyanide may coordinate first to ferric heme b_{595} instead of ferric heme *d*, because of its strong coordinating ability. Once such a species had been formed, the bound cyanide could not form a bridging structure and, at the same time, prevented the access of the second cyanide ion to ferric heme *d* due to steric hindrance. Such strong negative cooperativity between ligand binding to hemes *d* and b_{595} was proposed previously by Borisov *et al.* (*51*), and was inferred by us based on the results at studies on fluoride-binding to the air-oxidized enzyme (*17*). Thus, at an earlier stage after the addition of cyanide, a considerable amount of heme *d* remained in a 5-coordinated high-spin state (*i.e.*, the rhombic $g = 5.66$ high-spin species). The decrease in the rhombic high-spin signal in later stages, as the formation of the $g = 3.19$ species progressed, could be explained as the transfer of the bound cyanide from heme b_{595} to heme *d*, leading to an increase in the population of the reaction center having the cyanide-bridging structure. The concerted decreases in the intensity of the $g = 2.85$ species and the rhombic $g = 5.66$ high-spin species seemed consistent with this view. The transient $g = 2.96$ signal may also be due to the g_z component of the ferric heme b_{595}-cyanide species in which the heme *d* center in close proximity was in the reduced state.

Loehr, Gennis and coworkers proposed that cyanide-binding to ferric heme *d* leads a five-coordinated high-spin species, and attributed the features in the $g = 3.2$-2.8 region to ferric heme b_{558}, on the basis of the results of resonance Raman and EPR studies (*52, 53*). However, as demonstrated clearly in the present visible absorption study, the resultant ferric heme *d*-cyanide complex can be classified more likely as a 6-coordinated low-spin species. Their observation that "addition of cyanide to the fully oxidized enzyme results in a perturbation and net increase in intensity in the $g = 6$ region" is likely to be due to a higher population of the heme b_{595}-cyanide species in their sample upon the addition of cyanide, which may lead to the expulsion of a OH ligand from heme *d* due to the steric hindrance to form the 5-coordinated rhombic high-spin species.

Conclusions—Our present results established that cytochrome *bd* can bind azide, cyanide, and, to a lesser extent, thiocyanate at ferric heme *d*. Azide-binding caused the formation of a new EPR low-spin signal, as observed for other iron-chlorin-azide species, and the appearance of a visible absorption band at 647 nm. However, the FTIR data suggest that the binding configuration of azide seems anomalous, indicating some unknown effects of surrounding protein residues or ferric heme b_{595} in close proximity. Cyanide-binding was found to be very unusual. The spectral change upon cyanide-binding in the visible region was typical of those observed for ferric iron-chlorin species with diol substituents in macrocycles. However, there was no indication of the low-spin EPR signal typical of the ferric iron-chlorin-cyanide complex. Instead, derivative-shaped signals $g = 3.19$ and $g = 7.15$ derived from the heme *d*(Fe^{3+})-CN-heme b_{595}(Fe^{3+}) moiety appeared. This is consistent with the observation that the rhombic high-spin EPR signal (heme *d*) and the $g = 2.85$ species (heme b_{595}-cyanide) coexisted at an early stage after the addition of cyanide, but decreased at a later stage. Thus, the present study confirmed our previous proposal that heme *d* and heme b_{595} are located fairly close to each other.

REFERENCES

1. Jünemann, S. (1997) Cytochrome *bd* terminal oxidase. *Biochim. Biophys. Acta* **1321**, 107-127
2. Mogi, T., Tsubaki, M., Hori, H., Miyoshi, H., Nakamura, H., and Anraku, Y. (1998) Two terminal quinol oxidase families in *Escherichia coli*: Variations on molecular machinery for dioxygen reduction. *J. Biochem. Mol. Biol. Biophys.* **2**, 79-110
3. Miller, M.J. and Gennis, R.B. (1983) The purification and characterization of the cytochrome *d* terminal oxidase complex of the *Escherichia coli* aerobic respiratory chain. *J. Biol. Chem.* **258**, 9159-9165
4. Kita, K., Konishi, K., and Anraku, Y. (1984) Terminal oxidases of *Escherichia coli* aerobic respiratory chain II. Purification and properties of cytochrome b_{558}-*d* complex from cells grown with limited oxygen and evidence of branched electron-carrying systems. *J. Biol. Chem.* **259**, 3375-3381
5. Vavra, M.R., Timkovich, R., Yap, F., and Gennis, R.B. (1986) Spectroscopic studies on heme *d* in the visible and infrared. *Arch. Biochem. Biophys.* **250**, 461-468
6. Sotiriou, C. and Chang, C.K. (1988) Synthesis of the heme *d* prosthetic group of bacterial terminal oxidase. *J. Am. Chem. Soc.* **110**, 2264-2270
7. Timkovich, R., Cork, M.S., Gennis, R.B., and Johnson, P.Y. (1985) Proposed structure of heme *d*, a prosthetic group of bacterial terminal oxidases. *J. Am. Chem. Soc.* **107**, 6069-6075
8. Lorence, R.M. and Gennis, R.B. (1989) Spectroscopic and quantitative analysis of the oxygenated and peroxy states of the purified cytochrome *d* complex of *Escherichia coli*. *J. Biol. Chem.* **264**, 7135-7140
9. Kahlow, M.A., Loehr, T.M., Zuberi, T.M., and Gennis, R.B. (1993) The oxygenated complex of cytochrome *d* terminal oxidase: Direct evidence for Fe-O_2 coordination in a chlorin-containing enzyme by resonance Raman spectroscopy. *J. Am. Chem. Soc.* **115**, 5845-5846
10. Kahlow, M.A., Zuberi, T.M., Gennis, R.B., and Loehr, T.M. (1991) Identification of a ferryl intermediate of *Escherichia coli* cytochrome *d* terminal oxidase by resonance Raman spectroscopy. *Biochemistry* **30**, 11485-11489
11. Hata, A., Kirino, Y., Matsuura, K., Itoh, S., Hiyama, T., Konishi, K., Kita, K., and Anraku, Y. (1985) Assignment of ESR signals of *Escherichia coli* terminal oxidase complexes. *Biochim. Biophys. Acta* **810**, 62-72
12. Krasnoselskaya, I., Arutjunjan, A.M., Smirnova, I., Gennis, R., and Konstantinov, A.A. (1993) Cyanide-reactive sites in cytochrome *bd* complex from *E. coli*. *FEBS Lett.* **327**, 279-283
13. Hata-Tanaka, A., Matsuura, K., Itoh, S., and Anraku, Y. (1987) Electron flow and heme-heme interaction between cytochromes *b*-558, *b*-595 and *d* in a terminal oxidase of *Escherichia coli*. *Biochim. Biophys. Acta* **893**, 289-295
14. Hill, J.J., Alben, J.O., and Gennis, R.B. (1993) Spectroscopic evidence for a heme-heme binuclear center in the cytochrome *bd* ubiquinol oxidase from *Escherichia coli*. *Proc. Natl. Acad. Sci. USA* **90**, 5863-5867
15. D'mello, R., Palmer, S., Hill, S., and Poole, R.K. (1994) The cytochrome *bd* terminal oxidase of *Azotobacter vinelandii*: Low temperature photodissociation spectrometry reveals reactivity of cytochromes b_{595} and *d* with both carbon monoxide and oxygen. *FEMS Microbiol. Lett.* **121**, 115-120
16. Tsubaki, M., Hori, H., Mogi, T., and Anraku, Y. (1995) Cyanide-binding site of *bd*-type ubiquinol oxidase from *Escherichia coli*. *J. Biol. Chem.* **270**, 28565-28569
17. Tsubaki, M., Mogi, T., and Hori, H. (1999) Fluoride-binding to the *Escherichia coli bd*-type ubiquinol oxidase studied by visible absorption and EPR spectroscopies. *J. Biochem.* **126**, 98-103
18. Meinhardt, S.W., Gennis, R.B., and Ohnishi, T. (1989) EPR studies of the cytochrome-*d* complex of *Escherichia coli*. *Biochim. Biophys. Acta* **975**, 175-184
19. Rothery, R.A. and Ingledew, W.J. (1989) The cytochromes of anaerobically grown *Escherichia coli*. An electron-paramagnetic-resonance study of the cytochrome *bd* complex *in situ*. *Biochem. J.* **261**, 437-443
20. Iizuka, T. and Kotani, M. (1968) Analysis of a thermal equilibrium phenomenon between high-spin and low-spin states of ferrimyoglobin azide. *Biochim. Biophys. Acta* **154**, 417-419
21. Tsubaki, M. (1993) Fourier-transform infrared study of cyanide binding to Fe_{a3}-Cu_B binuclear site of bovine heart cytochrome *c* oxidase: Implication of the redox-linked conformational change at the binuclear site. *Biochemistry* **32**, 164-173
22. Tsubaki, M. (1993) Fourier-transform infrared study of azide binding to Fe_{a3}-Cu_B binuclear site of bovine heart cytochrome *c* oxidase: New evidence for the redox-linked conformational change at the binuclear site. *Biochemistry* **32**, 174-182
23. Alben, J.O. and Fager, L.Y. (1972) Infrared studies of azide bound to myoglobin and hemoglobin. Temperature dependence of ionicity. *Biochemistry* **11**, 842-847
24. Tsubaki, M., Hiwatashi, A., Ichikawa, Y., and Hori, H. (1987) Electron paramagnetic resonance study of ferrous cytochrome P-450_{scc}-nitric oxide complexes: Effects of cholesterol and its analogues. *Biochemistry* **26**, 4527-4534
25. Hori, H., Masuya, F., Tsubaki, M., Yoshikawa, S., and Ichikawa, Y. (1992) Electronic and stereochemical characterization of intermediates in the photolysis of ferric cytochrome P450scc nitrosyl complexes. Effects of cholesterol and its analogues on ligand binding structures. *J. Biol. Chem.* **267**, 18377-18381
26. Tsubaki, M., Uno, T., Hori, H., Mogi, T., Nishimura, Y., and Anraku, Y. (1993) Cytochrome *d* axial ligand of the *bd*-type terminal quinol oxidase from *Escherichia coli*. *FEBS Lett.* **335**, 13-17
27. Tsubaki, M., Mogi, T., Anraku, Y., and Hori, H. (1993) Structure of the heme-copper binuclear center of the cytochrome *bo* complex of *Escherichia coli*: EPR and Fourier-transform infrared spectroscopic studies. *Biochemistry* **32**, 6065-6072
28. Cheesman, M.R. and Walker, F.A. (1996) Low-temperature MCD studies of low-spin ferric complexes of tetramesitylporphyrinate: Evidence for the novel $(d_{xz},d_{yz})^4(d_{xy})^1$ ground state which models the spectroscopic properties of heme *d*. *J. Am. Chem. Soc.* **118**, 7373-7380
29. Hori, H., Tsubaki, M., Mogi, T., and Anraku, Y. (1996) EPR study of NO complex of *bd*-type ubiquinol oxidase from *Escherichia coli*: The proximal axial ligand of heme *d* is nitrogenous amino acid residue. *J. Biol. Chem.* **271**, 9254-9258
30. Stolzenberg, A.M., Strauss, S.H., and Holm, R.H. (1981) Iron(II, III)-chlorin and -isobacteriochlorin complexes. Models of the heme prosthetic groups in nitrite and sulfite reductases: Means of formation and spectroscopic and redox properties. *J. Am. Chem. Soc.* **103**, 4763-4778
31. Berzofsky, J.A., Peisach, J., and Blumberg, W.E. (1971) Sulfheme proteins I. Optical and magnetic properties of sulfmyoglobin and its derivatives. *J. Biol. Chem.* **246**, 3367-3377
32. Bracete, A.M., Kadkhodayan, S., Sono, M., Huff, A.M., Zhuang, C., Cooper, D.K., Smith, K.M., Chang, C.K., and Dawson, J.H. (1994) Iron chlorin-reconstituted histidine-ligated heme proteins as models for naturally occurring iron chlorin proteins: Magnetic circular dichroism spectroscopy as a probe of iron chlorin coordination structure. *Inorg. Chem.* **33**, 5042-5049
33. Koland, J.G., Miller, M.J., and Gennis, R.B. (1984) Potentiometric analysis of the purified cytochrome *d* terminal oxidase complex from *Escherichia coli*. *J. Biol. Chem.* **23**, 1051-1056
34. Loewen, P.C., Switala, J., von Ossowski, I., Hillar, A., Christie, A., Tattrie, B., and Nicholls, P. (1993) Catalase HPII of *Escherichia coli* catalyzes the conversion of protoheme to *cis*-heme *d*. *Biochemistry* **32**, 10159-10164
35. Peng, Q. and Peterson, J. (1994) The use of near-infrared charge-transfer transitions of low-spin ferric chlorins in axial ligand assignment. *FEBS Lett.* **356**, 159-161
36. Chatfield, M.J., La Mar, G.N., and Kauten, R.J. (1987) Proton NMR characterization of isomeric sulfmyoglobins: Preparation, interconversion, reactivity patterns, and structural features. *Biochemistry* **26**, 6939-6950
37. Jacob, G.S. and Orme-Johnson, W.H. (1979) Catalase of *Neurospora crassa*. 1. Induction, purification, and physical properties. *Biochemistry* **18**, 2967-2975

38. Sutherland, J., Greenwood, C., Peterson, J., and Thomson, A.J. (1986) An investigation of the ligand-binding properties of *Pseudomonas aeruginosa* nitrite reductase. *Biochem. J.* **233**, 893-898
39. Maj, M., Nicholls, P., Obinger, C., Hillar, A., and Loewen, P.C. (1996) Reaction of *E. coli* catalase HPII with cyanide as ligand and as inhibitor. *Biochim. Biophys. Acta* **1298**, 241-249
40. McCoy, S. and Caughey, W.S. (1970) Infrared studies of azido, cyano, and other derivatives of metmyoglobin, methemoglobin, and hemins. *Biochemistry* **9**, 2387-2393
41. Bogumil, R., Hunter, C.L., Maurus, R., Tang, H.-L., Lee, H., Lloyd, E., Brayer, G.D., Smith, M., and Mauk, A.G. (1994) FTIR analysis of the interaction of azide with horse heart myoglobin variants. *Biochemistry* **33**, 7600-7608
42. Watmough, N.J., Cheesman, M.R., Gennis, R.B., Greenwood, C., and Thomson, A.J. (1993) Distinct forms of the haem *o*-Cu binuclear site of oxidised cytochrome *bo* from *Escherichia coli*. Evidence from optical and EPR spectroscopy. *FEBS Lett.* **319**, 151-154
43. Little, R.H., Cheesman, M.R., Thomson, A.J., Greenwood, C., and Watmough, N.J. (1996) Cytochrome *bo* from *Escherichia coli*: Binding of azide to Cu_B. *Biochemistry* **35**, 13780-13787
44. Pate, J.E., Thamann, T.J., and Solomon, E.I. (1986) Resonance Raman studies of the coupled binuclear copper active site in met azide hemocyanin. *Spectrochim. Acta* **42A**, 313-318
45. Pate, J.E., Ross, P.K., Thamann, T.J., Reed, C.A., Karlin, K.D., Sorrell, T.N., and Solomon, E.I. (1989) Spectroscopic studies of the charge transfer and vibrational features of binuclear copper-(II) azide complexes: Comparison to the coupled binuclear copper active site in met azide hemocyanin and tyrosinase. *J. Am. Chem. Soc.* **111**, 5198-5209
46. Tsubaki, M., Mogi, T., and Hori, H. (1999) Fourier-transform infrared studies on azide binding to the binuclear center of the *Escherichia coli bo*-type ubiquinol oxidase. *FEBS Lett.* **449**, 191-195
47. Jacob, G.S. and Orme-Johnson, W.H. (1979) Catalase of *Neurospora crassa*. 2. Electron paramagnetic resonance and chemical properties of the prosthetic group. *Biochemistry* **18**, 2975-2980
48. Dawson, J.H., Bracete, A.M., Huff, A.M., Kadkhodayan, S., Zeitler, C.M., Sono, M., Chang, C.K., and Loewen, P.C. (1991) The active site structure of *E. coli* HPII catalase. Evidence favoring coordination of a tyrosinate proximal ligand to the chlorin iron. *FEBS Lett.* **295**, 123-126
49. Jünemann, S. and Wrigglesworth, J.M. (1995) Cytochrome bd oxidase from *Azotobacter vinelandii*. Purification and quantitation of ligand binding to the oxygen reduction site. *J. Biol. Chem.* **270**, 16213-16220
50. Peng, Q., Timkovich, R., Loewen, P.C., and Peterson, J. (1992) Identification of heme macrocycle type by near-infrared magnetic circular dichroism spectroscopy at cryogenic temperatures. *FEBS Lett.* **309**, 157-160
51. Borisov, V., Arutyunyan, A.M., Osborne, J.P., Gennis, R.B., and Konstantinov, A.A. (1999) Magnetic circular dichroism used to examine the interaction of *Escherichia coli* cytochrome *bd* with ligands. *Biochemistry* **38**, 740-750
52. Sun, J., Oscorne, J.P., Kahlow, M.A., Kaysser, T.M., Gennis, R.B., and Loehr, T.M. (1995) Resonance Raman studies of *Escherichia coli* cytochrome *bd* oxidase. Selective enhancement of the three heme chromophores of the "as-isolated" enzyme and characterization of the cyanide adduct. *Biochemistry* **34**, 12144-12151
53. Sun, J., Kahlow, M.A., Kaysser, T.M., Osborne, J.P., Hill, J.J., Rohlfs, R.J., Hille, R., Gennis, R.B., and Loehr, T.M. (1996) Resonance Raman spectroscopic identification of a histidine ligand of b_{595} and the nature of the ligation of chlorin *d* in the fully reduced *Escherichia coli* cytochrome *bd* oxidase. *Biochemistry* **35**, 2403-2412